

# A 15 cm aperture LED scintillometer for $C_n^2$ and crosswind measurements

W. Kohsiek

wetenschappelijke rapporten WR 87-3

scientific reports WR 87-3

Contents

1. Introduction	2
2. The scintillometer	2
3. Measurements	4
4. Results	5
4.1 Refractive index structure parameter	5
4.2 Crosswind	5
5. References	6
Appendix A Electronics	8
Appendix B Operation region	10

## 1. INTRODUCTION

An optical scintillometer was built to measure the refractive index structure parameter ( $C_n^2$ ) and the wind speed across the transmission path. The device uses a LED (light emitting diode) at 0.94  $\mu\text{m}$  as a light source and simple semiconductor light detectors. The aim of this report is to give a brief description of the scintillometer and some results we got with it on a test path of 449 m at Cabauw, The Netherlands.

## 2. THE SCINTILLOMETER

The scintillometer has been constructed after a design of Ochs and Cartwright, 1980<sup>a</sup>. It consists of a transmitter, a dual receiver and electronics for signal processing. We give some details:

Transmitter (Fig. 1). It uses a TIES-27 light emitting diode with a maximum optical output power of 15 mW at a current of 300 mA. In order to enhance background discrimination, the LED is switched on and off electronically at 1.6 kHz. The LED is placed in the focus of a spherical mirror with a focal length of 27.9 cm and a diameter of 15 cm. The effective aperture was measured by observing the relative radiation power at the receiver as function of the diameter of diaphragms placed in front of the transmitter. It was found to be 13.8 cm. Due to the small emitting surface of the LED, aiming of the transmitter has to be rather precise, within 2 mrad. A parabolical mirror instead of a spherical one did not give notable different results. A frosted glass may be put in front of the LED to relax the demands on aiming accuracy at the expense of a shorter maximum transmission path. By using a frosted glass the output of the transmitter is reduced by a factor of 50.

Receiver (Fig. 2). A dual receiver made of two identical telescopes is employed. Two telescopes are required for measuring crosswind, but only one is sufficient for measuring  $C_n^2$ . Each telescope consists of a spherical mirror with an effective diameter of 14.9 cm and 27.9 cm focal length and a photodiode (Oriel 7184-1) with a sensitive area of 5 mm<sup>2</sup>. In front of each detector cell an interference filter has been placed with a passband of 40 nm and a peak transmission of 70%. The centers of the two telescopes are separated by 18 cm. Aiming precision has to be better than 5 mrad.

Signal processing. Each signal is amplified and filtered. Next, the 1.6 kHz carrier is removed, and the modulation measured on a logarithmic scale. To obtain  $C_n^2$ , the two demodulated signals are subtracted, amplified and band pass filtered, and the differential signal is finally measured by a root-mean-square voltmeter. To obtain the crosswind, both demodulated signals are subjected to a process called clipping, pass a digital low pass filter and are correlated by a one-bit correlator. The value of the covariance function is measured at several time delays between the two signals and from these values and the time scale the crosswind ( $u_{\perp}$ ) is calculated. This technique is discussed by Ting-i Wang et al., 1981. Both  $\log C_n^2$  and  $u_{\perp}$  are available as analog signals on output jackets. Details of the electronics and calibration procedures can be found in Ochs and Cartwright, 1980<sup>a,b</sup>. The present electronics differs from the one of Ochs only by some minor details, which are discussed in Appendix A.

Operation and alignment procedures. Reference is again made to Ochs and Cartwright, 1980<sup>a</sup>. There are a few differences between the present instrument and the one reference is made to, viz.

- the LED is switched at 1.6 kHz instead of 25 kHz;
- the automatic gain control (AGC) has been replaced by a fixed gain;
- no visual signal detection (green LEDs) is available;
- the scale of the "panal" meter (inside the electronics box) is different.

Calibration. First, the  $C_n^2$  calibration is discussed. If transmitter and receiver apertures were equal ( $D$ ), and if the two receiving telescopes were tangent, then the log amplitude variance  $\sigma_{\chi}^2$  depends on  $D$ , path length  $L$  and  $C_n^2$  as

$$\sigma_{\chi}^2 = 0.364 D^{-7/3} L^3 C_n^2 . \quad (1)$$

However, the apertures are not all the same and the two receiving telescopes not tangent. No simple relation like (1) applies in such a case and the relation between  $\sigma_{\chi}^2$  and  $D$ ,  $L$  and  $C_n^2$  in principle has to be calculated numerically. For a 13.8 cm transmitter and two 14.9 cm diameter receiver telescopes separated by 18 cm we found that

$$\sigma_{\chi}^2 = 36.6 L^3 C_n^2 \quad (2)$$

holds for  $200 \text{ m} < L < 10000 \text{ m}$  with an error of 3% or less. Relation (2) is thus sufficiently accurate for practical application. As the relation between  $\sigma_x^2$  and  $L$  differs from that of Ochs and Cartwright, 1980<sup>a</sup> (which is based on Eq. (1)), their calibration procedure has to be modified accordingly. Their equation (7) now reads:

$$K = 0.0955 \times 10^6 L^{-3/2} . \quad (3)$$

For the present instrument, the relation between the gain  $K$  and the position of the potmeter  $P$  is

$$K = 5.27 \frac{100.18 - P}{4.7 + P} . \quad (4)$$

Combining (3) and (4) we get

$$P = \frac{100.18 - 85171 L^{-3/2}}{1 + 18121 L^{-3/2}} . \quad (5)$$

Next, the calibration of the optical crosswind measurement needs a comment. In the electronical design a distance between the two receiving telescopes of 15 cm is assumed, whereas the real distance is 18 cm for our instrument. Afterwards, we multiplied the readings of the crosswind by a factor of  $18/15 = 1.2$ . The justification of this correction is that the instrument senses the time that a turbulent structure takes to drift from one telescope to the other; this time is proportional to the separation distance of the telescopes.

## 2. MEASUREMENTS

In 1985 and 1986 measurements were made near the KNMI meteorological tower at Cabauw. The optical path was 449 m long and 4.33 m above the surface, and orientated  $157^\circ$ - $337^\circ$  (receiver at north end of the path). In-situ measurements were carried out about halfway the optical path, at the same height but about 1 m shifted to the east. Measurements of wind speed using a cup anemometer and of fast temperature fluctuations with fine platinum sensors (Kohsiek, 1987) were done in order to get checks on the optical measurements. Wind direction was obtained from a vane on a 10 m mast. Because the conversion of  $C_T^2$  to  $C_n^2$  involves a (usually small) humidity correction, also measurements of the Bowen

ratio, that is the ratio of the sensible and latent heat flux, were carried out. It can be shown that the humidity correction is related to the Bowen ratio (Wesely, 1976).

#### 4. RESULTS

##### 4.1 Refractive index structure parameter

Data are presented for three days in July 1985. The atmospheric stability varied from near-neutral to unstable, and there was no precipitation. Fig. 3. shows 10 minute averaged values. Although there is a considerable scatter, the overall impression is one of a good agreement between the optically measured values of  $C_n^2$  and the ones following from in-situ observations. These results confirm similar observations by Ting-i Wang et al., 1978.

##### 4.2 Crosswind

Crosswind measurements were done in the second half of 1985 and in the spring of 1986. The data has been divided into three classes:

- Westerly winds, no rain (Fig. 4);
- Easterly winds, no rain (Fig. 5);
- Westerly winds, raining (Fig. 6).

No selection on the basis of atmospheric stability was made. The data shown in the scatter plots was selected such as to get a more or less even cover over the range of wind speed. Fig. 4 shows that on the average the optical wind measurements are 6% below the in-situ ones. Part of this discrepancy may be attributed to overspeeding of the cup anemometer. Furthermore, the optical measurements are averages of the crosswind component, while the in-situ measurements represent the component of the average wind across the optical path, which is always somewhat larger than the former quantity. In view of these aspects, we think that the agreement between optical and in-situ measurements is satisfactory, with the exclusion of wind speeds less than  $2 \text{ m s}^{-1}$  where the optical measurements drop off too fast. This lack of response stems from limitations of the covariance technique. At very low (cross) wind speeds, the covariance function gets very broad, and its determination inaccurate due to atmospheric "imperfections" such as intermittency, changing wind direction etc. In order to prevent a "wandering around" of the optically

determined wind speed in those situations, the electronics impose a bias to zero to the measurements. The imperfect behaviour at low wind speed is even more pronounced in Fig. 5, which refers to easterly winds. The asymmetrical behaviour at low wind speed regarding easterly winds and westerly winds is not well understood. Fig. 5 further shows that the optical crosswind is somewhat smaller than the in-situ crosswind, like Fig. 4. It should be noted that the data for easterly winds is less reliable than that for westerly winds because the light path was situated 30 m west from the 200 m mast and its obstructing building.

The comparison between optically inferred and in-situ measured crosswind is hardly or not affected by rain (Fig. 6). Rain introduces extra variance on the radiation received, but at higher frequencies than the variance occasioned by refractive index fluctuations (Ting-i Wang et al., 1982). These high frequency contributions are rejected by the electronical filters, which explains for the insensitivity of the scintillometer to rain.

A small set of data was analysed for checking the cosine response of the optical crosswind instrument. Figure 7 displays the ratio of the optical crosswind to the windspeed measured with a cup anemometer, as a function of the wind direction. The deviations as compared to a perfect cosine response are small. The above results demonstrate the capability of the scintillometer to measure crosswind, and should be regarded as an addition to many other reports on wind measurements by means of scintillation. A useful entrance to this body of literature is an article by Ochs and Ting-i Wang, 1978.

## 5. REFERENCES

- W. Kohsiek (1987): A device for measuring fast temperature fluctuations. KNMI Technical Report TR 92.
- G.R. Ochs and Ting-i Wang (1978): Finite aperture optical scintillometer for profiling wind and  $C_n^2$ . Appl. Optics 17, 3774-3778.
- G.R. Ochs and W.D. Cartwright (1980<sup>a</sup>): Optical system model VI for space-averaged wind and  $C_n^2$  measurements. NOAA Technical Memorandum ERL WPL-52.
- G.R. Ochs and W.D. Cartwright (1980<sup>b</sup>): A crosswind measurement module for the model II optical  $C_n^2$  instrument. NOAA Technical Memorandum ERL WPL-53.

Ting-i Wang, G.R. Ochs and S.F. Clifford (1978): A saturation-resistant optical scintillometer to measure  $C_n^2$ . J. Opt. Soc. Am. 68, 334-338.

Ting-i Wang, G.R. Ochs and R.S. Lawrence (1981): Wind measurements by the temporal cross-correlation of the optical scintillations. Appl. Optics 20, 4073-4081.

Ting-i Wang, R. Lataitis, R.S. Lawrence and G.R. Ochs (1982): Laser weather identifier: present and future. J. Appl. Meteorol. 21, 1747-1753.

M.L. Wesely (1976): The combined effect of temperature and humidity fluctuations on refractive index. J. Appl. Meteorol. 15, 43-49.



## APPENDIX A

Electronics

1. Light emitting diode driver circuit (schematic: see O&C\*)  
An extra 18 k $\Omega$  resistor has been added in series with the 10 k $\Omega$  frequency adjustment potmeter in order to accommodate for a 1.6 kHz wave. The FM option is not used.
2. Photodiode preamplifier (schematic 1)  
The preamp and photodiode is integrated in one package.
3. Automatic gain control circuit (schematic 2)  
The AGC provision has been omitted by taking out the FETs from the original circuit of O&C. We did so because the FETs may induce non-linear effects at certain signal levels. In order to accommodate for various light levels, feed-back resistors can be inserted in the sockets meant for the FETs in a rather simple way. For a fixed path length there is no need to change the feed-back resistors once a proper choice is made. A proper choice is such as to have an amplitude of about 1 V for the square wave at the jacket labelled "CARRIER".
4. Demodulator (schematic 3)  
The bandpass filter of O&C has been replaced by a two stage amplifier with weak low pass filtering characteristics. Rigorous filtering is postponed till the  $C_n^2$  circuit. This conforms later versions of the WPL scintillometer (Ochs, private comm.). The coupling capacitor to pin 1 of the AD536 has been chosen 10 nF instead of 100 nF. At high modulation levels it was found that the voltage at the linear output of the AD536 depends weakly on the value of the coupling capacitor. We found 10 nF to be an optimum value.

\* Ochs and Cartwright, 1980<sup>a</sup>.

5.  $C_n^2$  circuit (schematic: see O&C)

The present circuit is the same as that of O&C, with the exception of the value of the coupling capacitors, viz. 6.8  $\mu$ F instead of 10  $\mu$ F. In this circuit the difference of the demodulated signals passes through an active bandpass filter (3 dB points at 0.34 Hz and 400 Hz) that determines the frequency window of the detected scintillations.

6. Covariance analyzer circuit 1 (schematic 4)

The original circuit of O&C includes an active two stage high pass filter preceeding the clipping amplifier. In the present circuit the first high pass filter has been replaced by a low pass filter with cut off at 400 Hz. This makes the filtering identical to the one of the  $C_n^2$  circuit.

7. Covariance analyzer circuit 2 (schematic: see O&C)

We added a switch to the circuit board that connects the anodes of the two diodes connection to pin 6 of up amp JJ. This switch serves for testing purposes only and normally should be left open because otherwise the servo characteristic of the circuit deteriorates.

8. Circuit board lay outs. See O&C.

## APPENDIX B

Operation region

Figure 8 illustrates the values of  $C_n^2$  that can be measured as a function of path length  $L$ . The boundaries of the region of operation are determined by noise of the electronics, detector noise and scintillation saturation. The figure has been constructed for a dewpoint temperature of 10 °C. A different water vapour concentration will affect the position of the line labelled "LOW SIGNAL" because of a different absorption of radiation by water vapor (e.g. for a 10 km path the transmission is 10%). Other factors like haze or fog may dominate the transmission; these effects have not been taken into account. Saturation occurs at values of  $\sigma_T^2 = 0.124 k^{7/6} L^{11/6} C_n^2 > 0.191 (D\sqrt{\lambda L})^{5/3}$ . In the saturation region  $C_n^2$  is no longer directly proportional to  $\sigma_\chi^2$ . Values of  $C_n^2$  encountered in the atmospheric boundary layer range from  $10^{-12} \text{ m}^{-2/3}$  (close to the ground) down to  $10^{-16} \text{ m}^{-2/3}$  or less during short periods of time when the atmospheric stability changes from unstable to stable, or the reverse. It follows that useful pathlengths range from 200 m to 10 km, depending on the situation.

Regarding the measurement of crosswind, the same noise imposed limits can be considered as for the  $C_n^2$  measurement. However, saturation does not affect the crosswind measurement performance. Thus, under conditions of excellent visibility, the crosswind measurement facility could be used for paths well over 10 km. As a rule of thumb, the  $C_n^2$  measurement and the crosswind measurement both require a visibility that at least equals the path length.



Figure 1. The transmitter. The aperture has been stopped down to 5 cm.



Figure 2. The receiver. Apertures have been stopped down to 5 cm here.

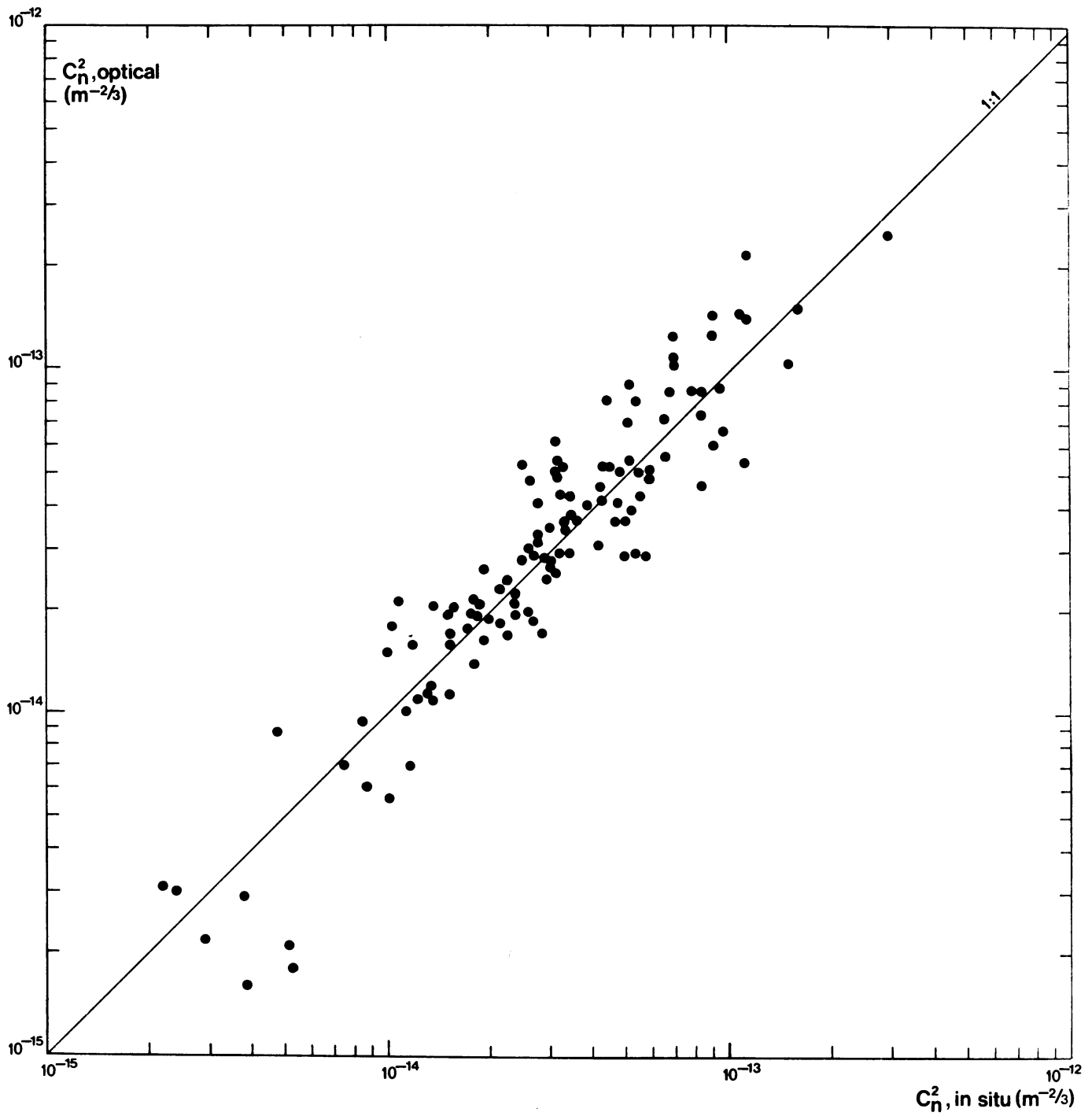


Figure 3. Comparison of optical measurements of  $C_n^2$  and in-situ measurements, 10 minutes averaged values.

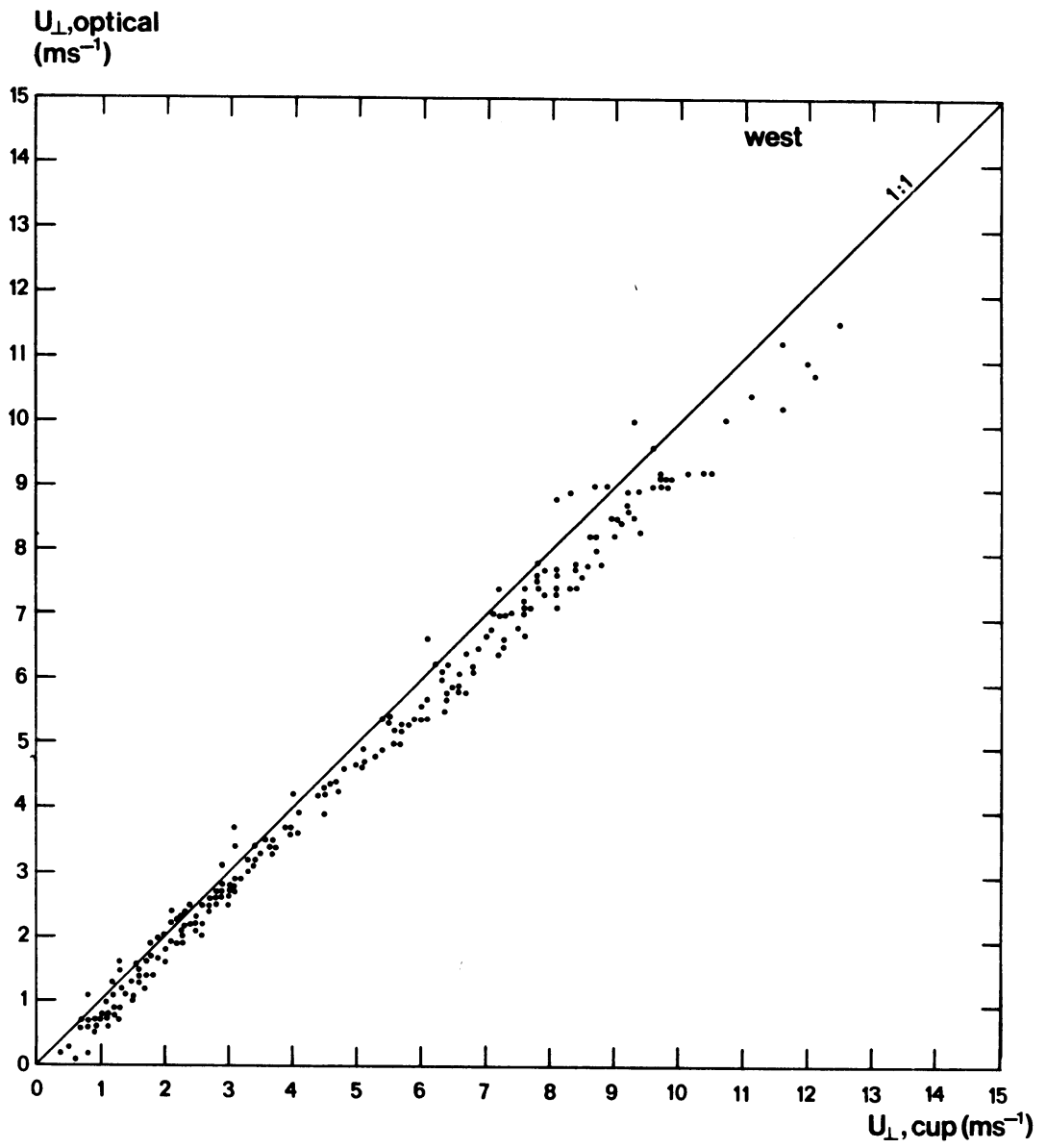


Figure 4. Comparison of optical measurement of crosswind and in-situ measurements, 10 minutes averaged values. Westerly winds.

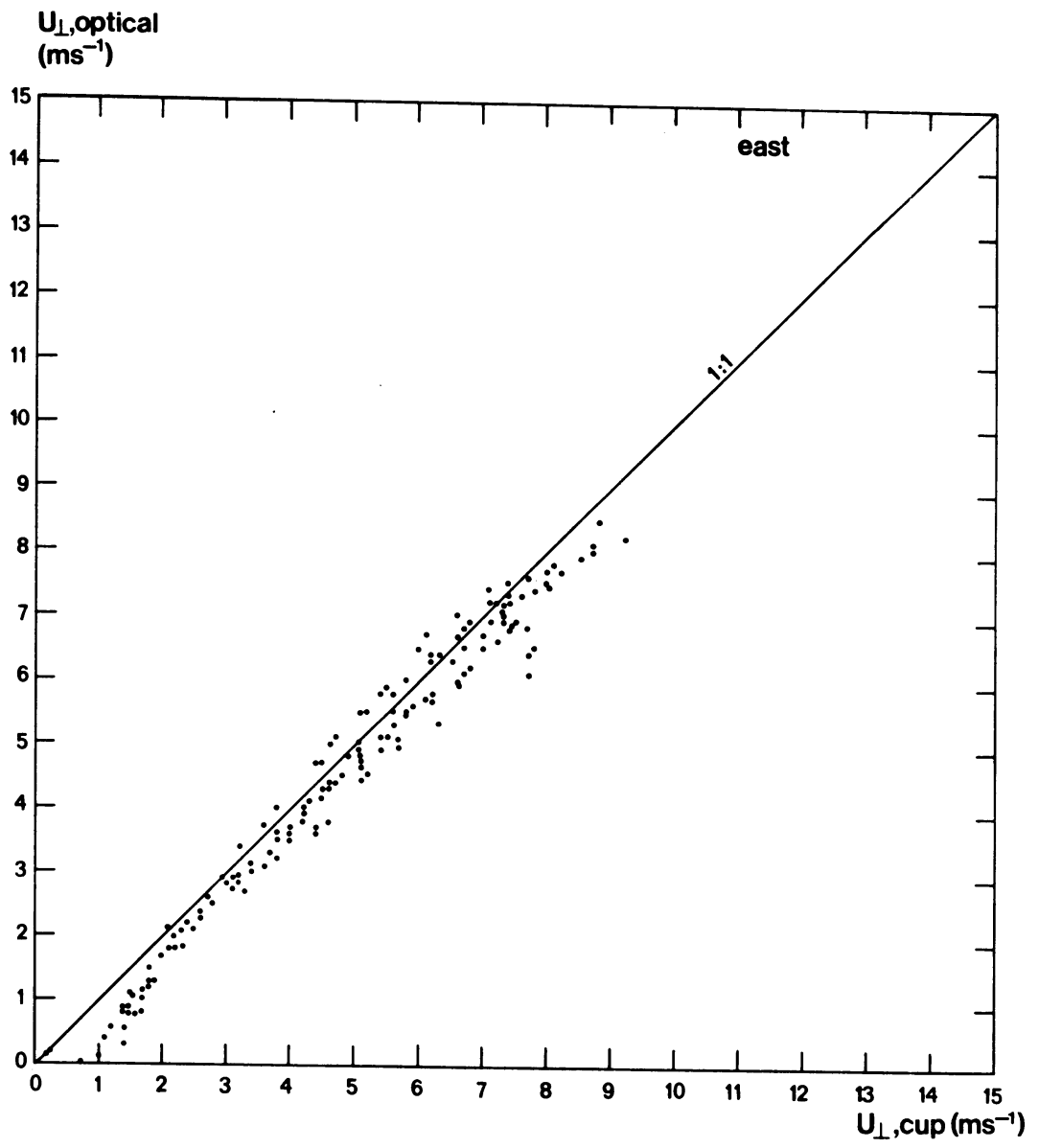


Figure 5. As Fig. 4, but easterly winds.



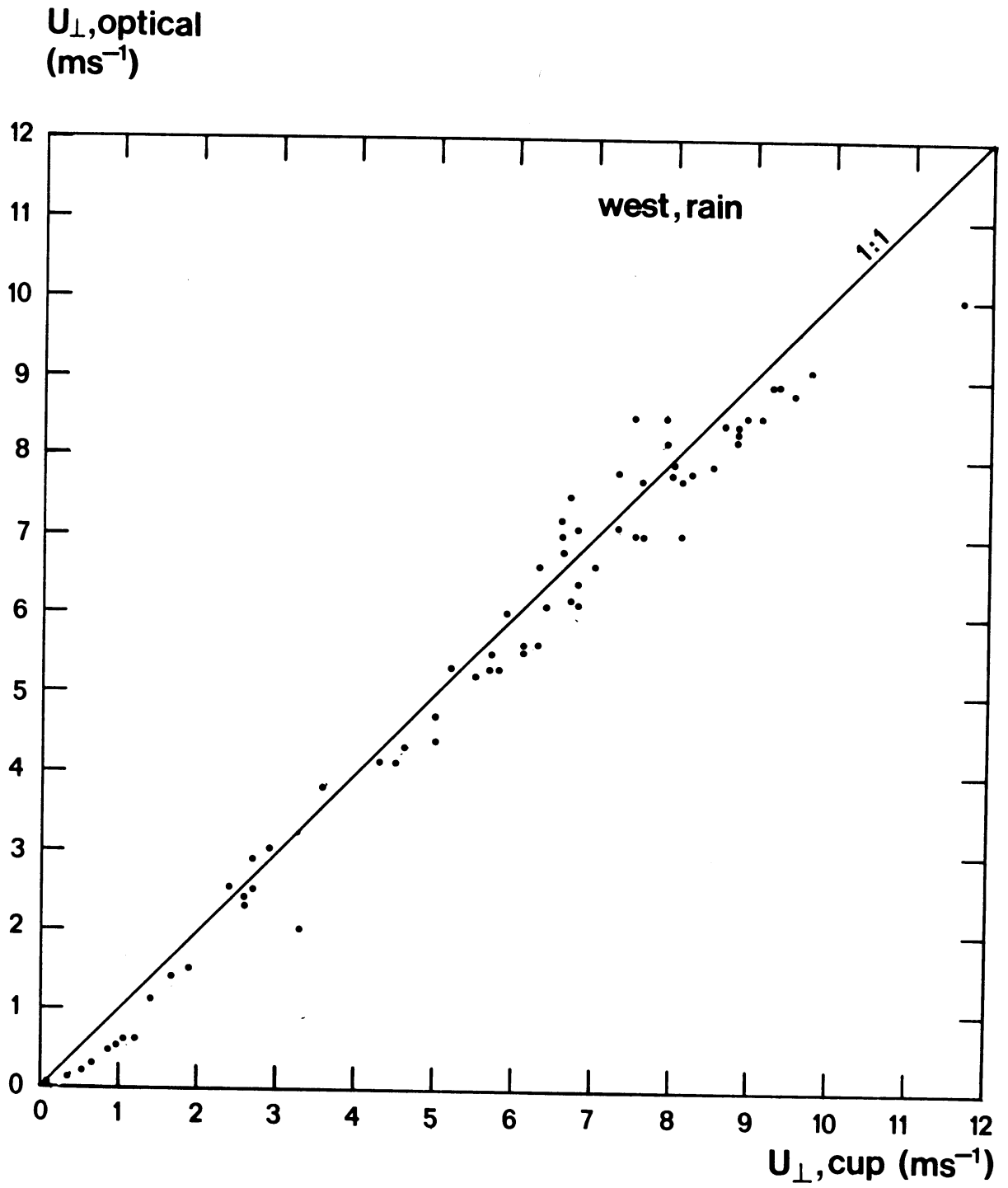


Figure 6. As Fig. 4, westerly winds, during rainfall.

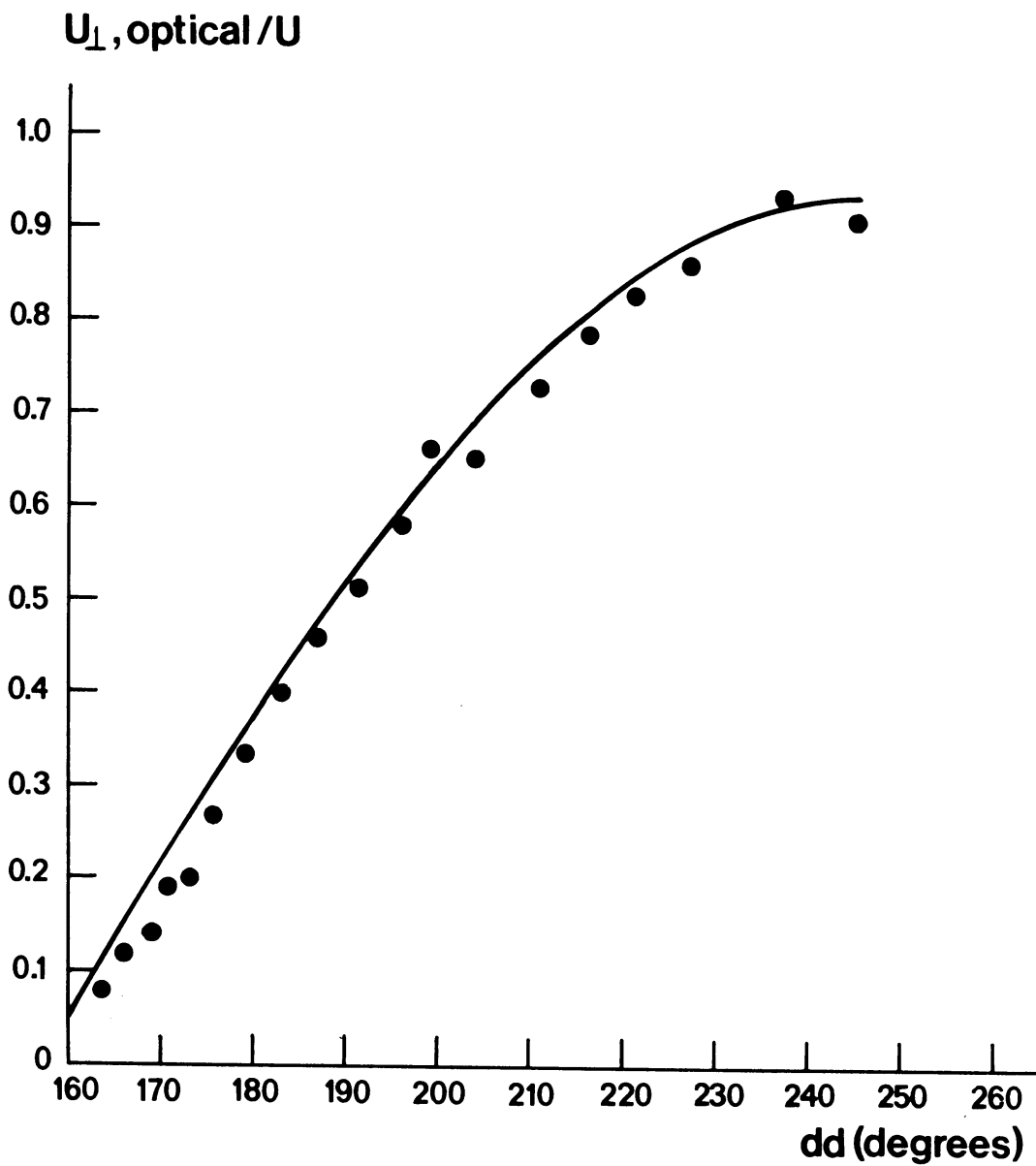


Figure 7. Ratio of the optical crosswind and the wind speed (cup anemometer) as function of wind direction (dots). The reference line represents  $0.94 \times \sin (dd + 23^\circ)$ .

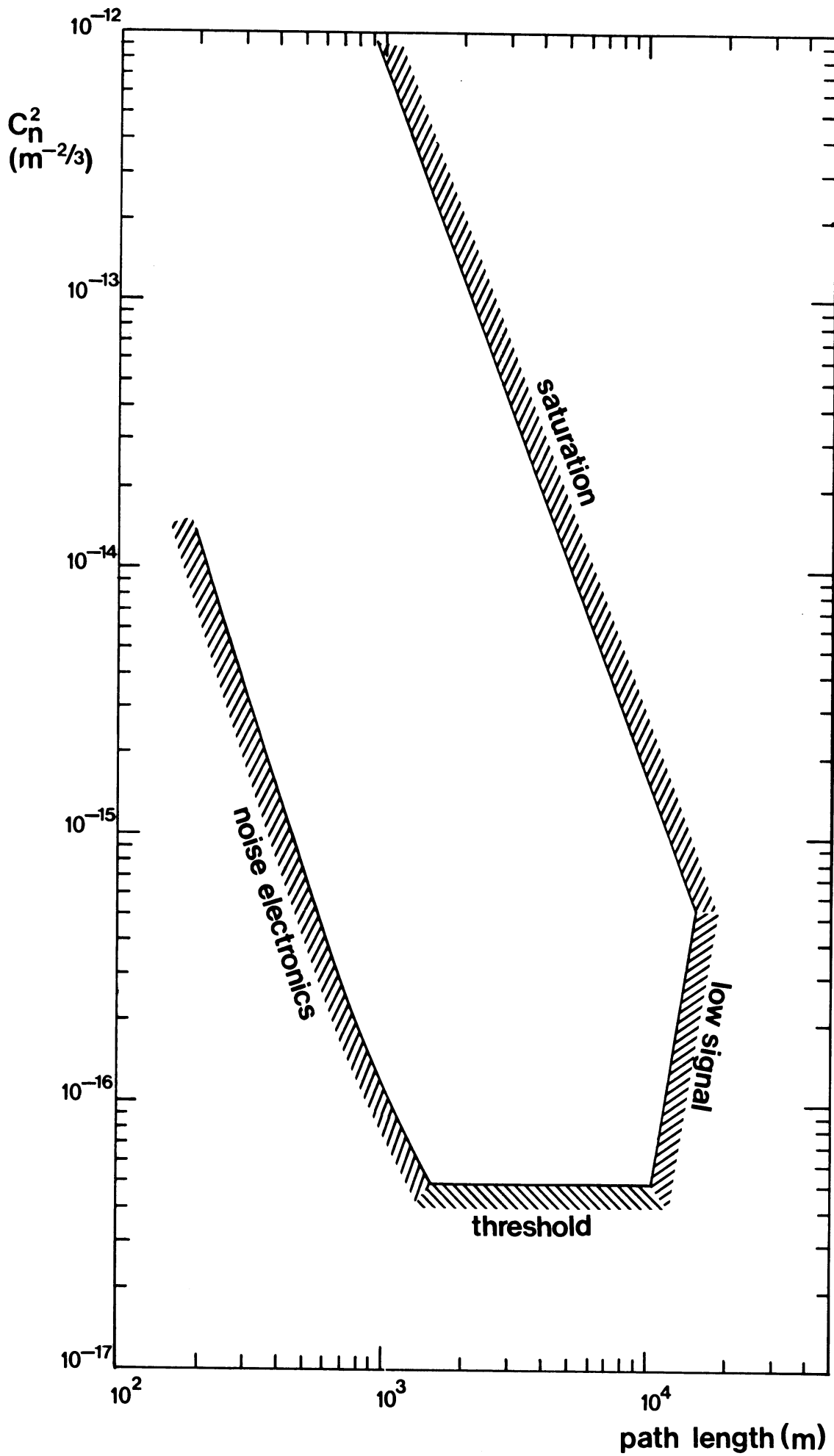
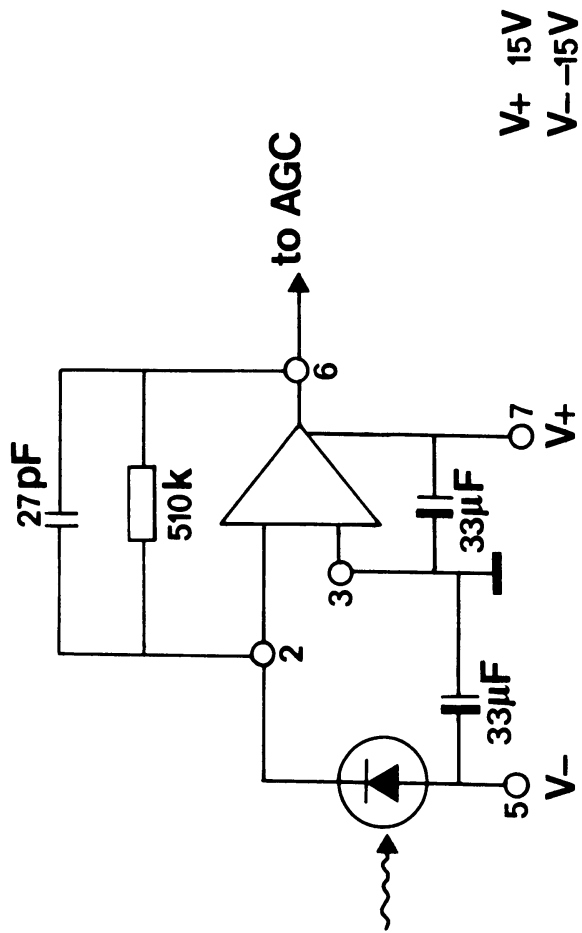
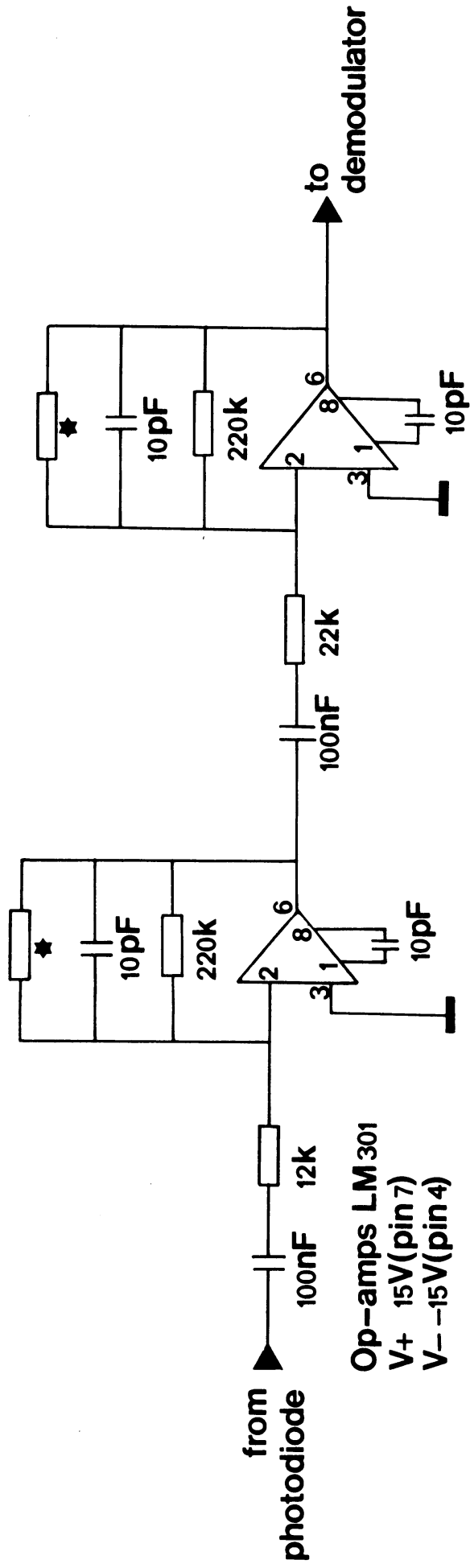


Figure 8. Region of operation of the 15 cm aperture LED scintillometer.



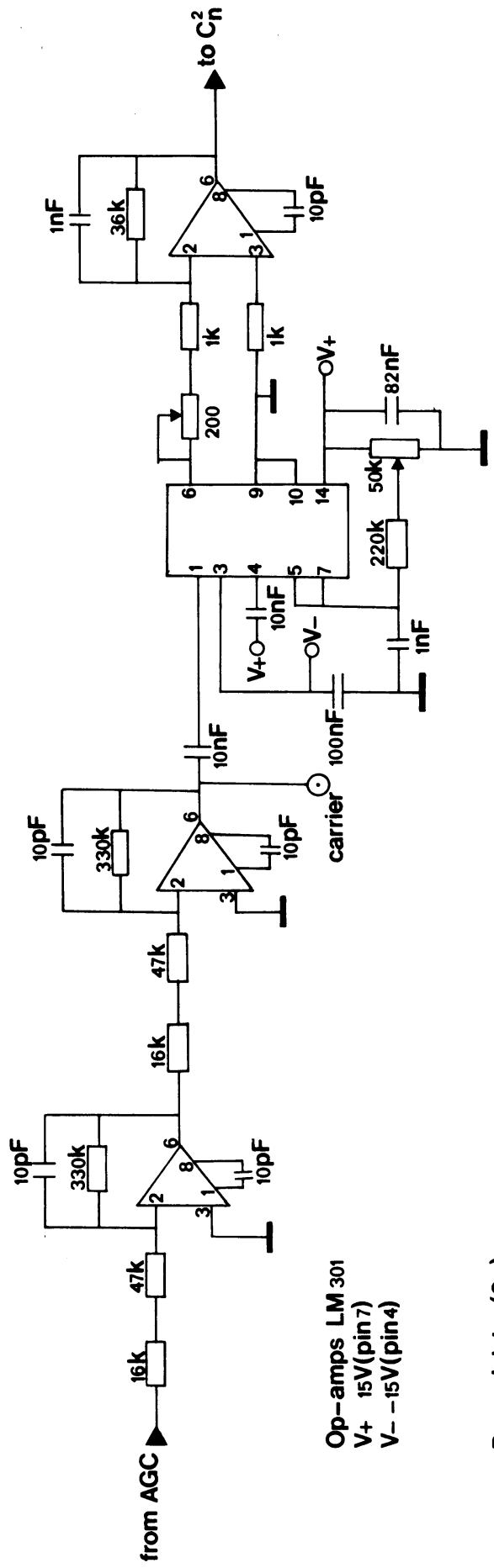
### Photodiode (2x)

Schematic 1. Photodiode preamplifier



★ resistors to be adjusted according to signal level  
 also capacitors may be inserted

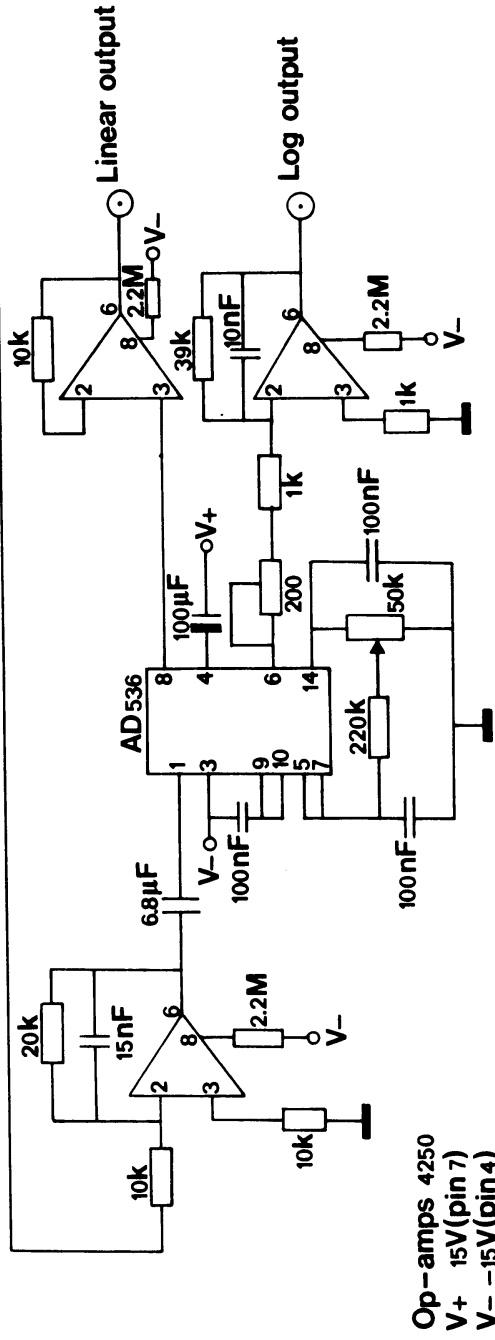
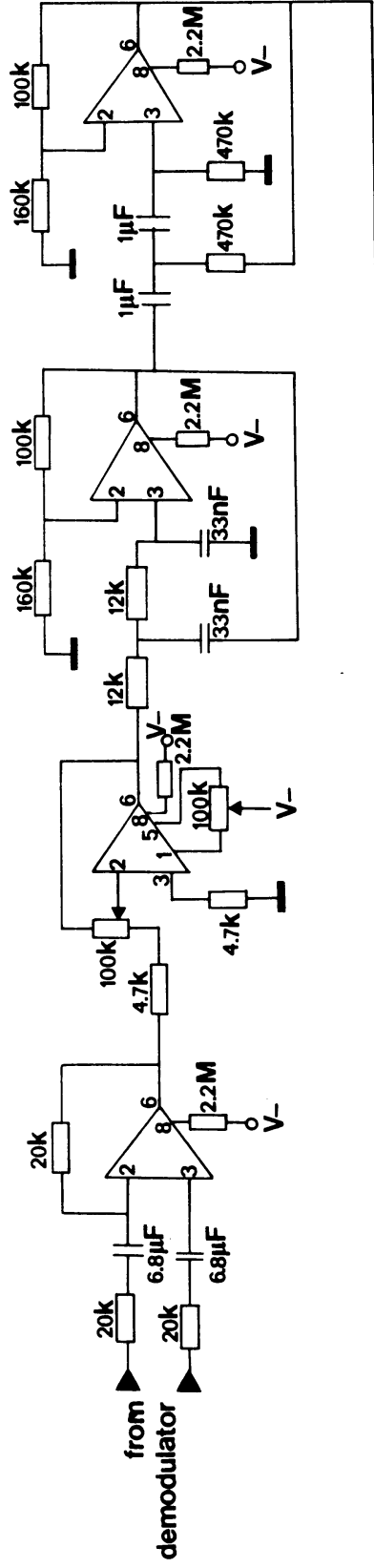
AGC (2x)



Op-amps LM 301  
 V+ 15V(pin 7)  
 V- -15V(pin 4)

Demodulator (2x)

Schematic 3. Demodulator



Op-amps 4250  
 V+ 15V (pin 7)  
 V- -15V (pin 4)

C<sub>n</sub> module

Schematic 4. C<sub>n</sub><sup>2</sup> circuit